PP/PE Blends by Reactive Extrusion: PP Rheological Behavior Changes

DIDIER GRAEBLING,[1] MORAND LAMBLA,[1] H. WAUTIER[2]

[1] Université Louis Pasteur/ECPM, Laboratoire d'Extrusion Réactive, 4, rue Boussingault, 67000 Strasbourg, France

[2] Solvay S.A. Laboratoire Central, rue de Ransbeek 310, 1120 Bruxelles, Belgique

Received 29 December 1996; accepted 16 January 1997

ABSTRACT: The aim of this work was to obtain a polypropylene (PP) with strain hardening in elongational flow by a reactive extrusion process. This rheological behavior imposes a structural modification of the PP: linear chain to long side branches. Reactive extrusion allows the modification of PP by radical chemistry, but this modification is accompanied by significant degradation of chains: β-scission. A polyfunctional monomer (TMPTA) associated with addition of polyethylene (PE) allows us to limit this degradation and to build a connected structure. Gel permeation chromatography measurements confirm the presence of high-molecular-weight species. With thermal analysis of modified polymers, we show the creation of copolymer PP/PE at the interface of the PE inclusions. Under these conditions, all the reactive blends present strain hardening. The elongational viscosity of all blends can be described by the Leonov model calculated with viscoelastic data. This model gives a good description of the viscosity without adjusted parameters. © 1997 John Wiley & Sons, Inc. J Appl Polym Sci **66:** 809–819, 1997

Key words: PP/PE blends; reactive extrusion; β-scission; high melt strength; structure/properties relationship

INTRODUCTION

Reactive extrusion is a classical method of macromolecular functionalization and of elaboration of compatibilized polymer blends. Various approaches used for blends preparation can be employed for structural modification of polymers. The molecular rearrangement of the chain is of interest when one wishes to modify the rheological behavior of a polymer in the molten state.

The aim of this work was to obtain polypropylene (PP) with strain hardening in elongational flow (PP-HMS: polypropylene high melt strength) by a reactive extrusion process. Reactive extrusion allows the modification of PP by radical chemistry, but this modification is accompanied by important degradation of chains by β-scission.

For a polymer in the molten state, two types of behavior in a steady uniaxial extension are typically observed:

- Troutonian behavior, corresponding to a steady stress regime, generally, for small strain rates;
- High melt strength or strain hardening, corresponding to a flow stabilization by stress increasing.

The high melt strength is obtained for materials with long side branches (polyethylene; PE) or for high molecular weight (polystyrene; PS). PP is a linear chain, it does not present this behavior

Correspondence to: D. Graebling.

Journal of Applied Polymer Science, Vol. 66, 809–819 (1997)
© 1997 John Wiley & Sons, Inc. CCC 0021-8995/97/050809-11

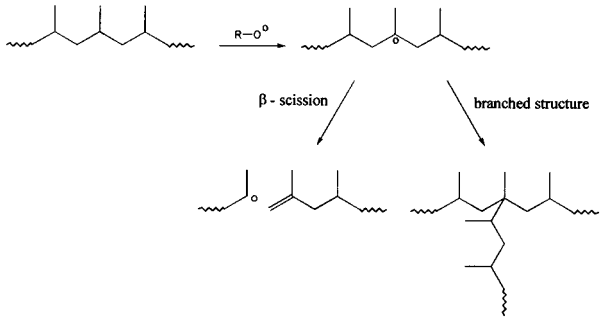

Figure 1 Competition between β-scission and polymer crosslinking.

in the range of the strain rate used for foaming or thermoforming processes. With a linear macromolecule, two approaches allow the transition of a flow regime to another for the same deformation rate: an increase of molecular weight or the creation of long side branches.

In order to obtain a polypropylene HMS, this polymer must contain some chains with long branches and high molecular weight. This condition, associated with the polymer structure, imposes the following chemical considerations:

- Reduced chain degradation;
- The creation of high molecular weight species with long branches and adequate concentration.

It is necessary to build the branched molecular structure from that destroyed by β-scission via a polyfunctional monomer (Fig. 1). The envisaged chemical modification must allow the grafting reaction between the polymer chains as compared with the β-scission reaction. Another difficulty of free-radical grafting arises from the competition between monomer grafting and homopolymerization.

CHEMICAL MODIFICATION

Structural Modification of PP

Flat has shown that it is possible to obtain an amorphous PP by reaction with bromomaleic anhydride (BRMA).[1,2] The substitution of one of the hydrogen atoms of maleic anhydride by bromine, which is electron-attracting, renders its double bond unsymmetrical, therefore increasing its reactivity towards free radicals. Added to increased reactivity are the thermally induced free radicals Br° as a result of the decomposition of the C—Br bond. The presence of Br° causes a decrease in the instantaneous concentration of free radicals and thus limits the β-scission. The decrease of molecular weight is limited. The emission of HBr during the chemical modification shows that the Br° can attack the hydrocarbon skeleton. The BRMA modifies the PP tacticity by inversion of the asymmetrical carbon configuration, leading to loss of crystallinity. The rheological dynamic measurements do not show the macroradical recombination. Thus, the PP is always linear.

To limit the degradation reaction of PP, different solid-state processes have been developed.

Borsig investigated the role of polyfunctional monomers such as pentaerythritol tetra allyl ether (PETA), with peroxide in raising the crosslinking efficiency of PP.[3] Polyfunctional grafted to PP is an active site for trapping another macroradical and for formation of a crosslinked structure by connecting the chains. Borsig has prepared crosslinked PP by modification in the solid state at 170°C. At this temperature, the degradation is limited by the small mobility of polymer chains.

In a patent application filed on behalf of the Himont Company by De Nicola, modification of PP in the solid state is made with peroxide in the absence of oxygen in order to obtain branched macromolecules and gel-free polymer.[4] This modification is realized in several steps to temperatures comprising between 70 and 150°C, therefore at temperatures below the melting point of PP, in the absence of oxygen. Two types of peroxide are employed, one decomposing at low temperature (half-life time $\approx$ 30 s/100°C), the other at higher temperature (half-life time $\approx$ 30 s/135°C). No coupling agent was employed. The examples of this patent show that high melt strength is obtained and that the molecular weight is greater than the initial PP.

PP/PE Blends

The addition of PE during the chemical modification of PP can be envisaged as a way of reducing the β-scission. Yu studied the effect of the peroxide concentration on the rheological behavior and weight distribution of PP/low-density PE (LDPE) blends.[5] A blend of PP/LDPE 75/25 is characterized by strain hardening as a result of partial crosslinking of the LDPE phase.

Chodak used, in the case of PP/LDPE blends, a peroxide with a quinone that slightly delays the crosslinking of the PE and activates the crosslinking process of PP.[6]

Borsig envisaged the crosslinking of PP/PE blends in all concentration ranges of polymer, with a peroxide and PETA as polyfunctional monomer.[7] This coagent seems more reactive with PE than PP.

RHEOLOGY

Structure/Properties Relationship

A simple rheological model like Lodge's model can be used for relating the rheological behavior in a steady unixial extension to polymer structure. For this model, and taking into account that the memory function is one relaxation time, Maxwell liquid λ, the elongational viscosity expression is

$$\eta_e^+(t, \dot{\varepsilon}) = \frac{2\eta}{1 - 2\dot{\varepsilon}\lambda}\left(1 - \exp\left(-\frac{1 - 2\dot{\varepsilon}\lambda}{\lambda}t\right)\right) + \frac{\eta}{1 + \dot{\varepsilon}\lambda}\left(1 - \exp\left(-\frac{1 + \dot{\varepsilon}\lambda}{\lambda}t\right)\right) \quad (1)$$

In a steady regime, this expression reduces to

$$\eta_e^+(\dot{\varepsilon}) = \lim_{t\to\infty} \eta_e^+(t, \dot{\varepsilon}) = \frac{3\eta}{(1 - 2\dot{\varepsilon}\lambda)(1 + \dot{\varepsilon}\lambda)} \quad (2)$$

The elongational viscosity diverges when $\dot{\varepsilon} \geq 1/2\lambda$ (i.e., for a strain rate inversely proportional to the characteristic time of the Maxwell model). The Troutonian regime is obtained when the strain rate approaches zero:

$$\eta_e = \lim_{\substack{t\to\infty \\ \dot{\varepsilon}\to 0}} \eta_e^+(t, \dot{\varepsilon}) = 3\eta \quad (3)$$

One can make an analogy between the polymer terminal relaxation time τ_w and the relaxation time of the Maxwell model λ. The relaxation time increases more quickly with the molecular weight for a branched chain than for a linear chain (Table I). The grafting is preferable to an increase of molecular weight, to limit the increase of the shear viscosity.

Table I Comparison Between Linear Chain and Branched Chain

	Linear Chain	Branched Chain
η_0	$K M^{3,4}$	$K'' M^{\alpha}$ with $\alpha > 3, 4$
J_e^0	Const.	βM
τ_W	$\eta_0^L \times J_e^{0\,L} = K' M^{3,4}$	$\eta_0^B \times J_e^{0\,B} = K''' M^{\alpha+1}$

Several papers[8–11] give the rheological behavior of branched PPs. All these polymers show strain hardening in uniaxial elongational measurements. They are characterized by a large molecular weight distribution and very long terminal relaxation time.

According to Gaylord,[12] the PP HMS is characterized by a bimodal molecular weight distribution, wherein the higher molecular weight fraction contains branched polymer. He gives the following molecular weight and rheological characterization of this PP:

- $M_z \geq 10^6$ and $M_z/M_w \geq 3$
- $J_e^0 \geq 1.2 \times 10^{-5}\text{Pa}^{-1}$.

Leonov Model

Leonov's approach is to relate the stress tensor to the elastic strain stored in the material.[13–18]

In the single-mode version, the stored elasticity is precisely the strain that would be recovered if all loads were suddenly removed from the sample. In shearing, the elastic strain is not the same as the recoverable shear because the normal stresses are not removed.

The elastic strain, according to Leonov, is a tensor that describes the change in shape of the material element in free recovery. This evolution can be described by a Finger tensor that represents the elastic strain tensor of Leonov. The Leonov constitutive equation is

$$\overset{\nabla}{\underline{\underline{C}}}_e^{-1} + \frac{1}{2\lambda}\{\underline{\underline{\hat{C}}}_e^{-1} - \underline{\underline{\hat{C}}}_e\} \times \underline{\underline{C}}_e^{-1} = \underline{\underline{0}}$$

$$\underline{\underline{\tau}} = G\underline{\underline{C}}_e^{-1} \quad (4)$$

with

$$\underline{\underline{\hat{C}}}_e^{-1} = \underline{\underline{C}}_e^{-1} - \tfrac{1}{3} tr\{\underline{\underline{C}}_e^{-1}\}\underline{\underline{\delta}}$$
$$\underline{\underline{\hat{C}}}_e = \underline{\underline{C}}_e - \tfrac{1}{3} tr\{\underline{\underline{C}}_e\}\underline{\underline{\delta}} \quad (5)$$

In the case of a steady unixial extension, the strength κ of a material is the sum of two contributions, recoverable elastic extension κ_e and not recoverable κ_p:

$$\kappa = \frac{l(t)}{l_0} \quad \kappa_e = \frac{l(t)}{l_p(t)} \quad \kappa_p = \frac{l_p(t)}{l_0} \quad (6)$$

The deformation tensor $\underline{\underline{F}}_e^{-1}$ associated with the elastic term, for an elongational flow and an incompressible media is

$$\underline{\underline{F}}_e^{-1} = \begin{vmatrix} \kappa_e^2 & 0 & 0 \\ 0 & \kappa_e^{-1/2} & 0 \\ 0 & 0 & \kappa_e^{-1/2} \end{vmatrix} \quad (7)$$

The Finger tensor and the Cauchy tensor are

$$\underline{\underline{C}}_e^{-1} = \begin{vmatrix} \kappa_e^2 & 0 & 0 \\ 0 & \kappa_e^{-1} & 0 \\ 0 & 0 & \kappa_e^{-1} \end{vmatrix} \quad \underline{\underline{C}}_e = \begin{vmatrix} \kappa_e^{-2} & 0 & 0 \\ 0 & \kappa_e & 0 \\ 0 & 0 & \kappa_e \end{vmatrix} \quad (8)$$

For this flow, the rate of deformation tensor is written as

$$\underline{\underline{D}} = \begin{vmatrix} \dot{\varepsilon} & 0 & 0 \\ 0 & -\dot{\varepsilon}/2 & 0 \\ 0 & 0 & -\dot{\varepsilon}/2 \end{vmatrix} \quad (9)$$

Moreover, this flow is characterized by an absence of vorticity and eq. (4) then becomes

$$\frac{\partial}{\partial t}\underline{\underline{C}}_e^{-1} - 2\,\underline{\underline{C}}_e^{-1} \times \underline{\underline{D}} + \frac{1}{2\lambda}\{\underline{\underline{\hat{C}}}_e^{-1} - \underline{\underline{\hat{C}}}_e\} \times \underline{\underline{C}}_e^{-1} = \underline{\underline{0}}$$
$$\underline{\underline{\tau}} = G\underline{\underline{C}}_e^{-1} \quad (10)$$

From expressions of the different tensors given in eqs. (8) and (9), we obtain

$$\frac{6\lambda}{\kappa_e}\frac{\partial}{\partial t}\kappa_e - 6\dot{\varepsilon}\lambda + (\kappa_e^2 + \kappa_e^{-1})(1 + \kappa_e^{-1}) = 0 \quad (11)$$

For solving this differential equation by the Runge–Kutta method, it is preferable to write this relationship in the following form:

$$\frac{\partial}{\partial t}\kappa_e = \dot{\varepsilon}\kappa_e - \frac{\kappa_e}{6\lambda}(\kappa_e^2 + \kappa_e^{-1})(1 + \kappa_e^{-1}) \quad (12)$$

A unixial extension measurement gives the elongational viscosity $\eta_e^+(\dot{\varepsilon}, t)$:

$$\eta_e^+(\dot{\varepsilon}, t) = \frac{\tau_{11}(\dot{\varepsilon}, t) - \tau_{22}(\dot{\varepsilon}, t)}{\dot{\varepsilon}} = \frac{\sigma_{11}(\dot{\varepsilon}, t) - \sigma_{22}(\dot{\varepsilon}, t)}{\dot{\varepsilon}} \quad (13)$$

$$\eta_e^+(\dot{\varepsilon}, t) = \frac{\eta}{\dot{\varepsilon}\lambda}[\kappa_e^2(\dot{\varepsilon}, t) - \kappa_e^{-1}(\dot{\varepsilon}, t)] \quad (14)$$

The rheological behavior of a polymer in a molten state cannot be described by a single-mode model. The Leonov model is easily extended to the multimode case. For each mode i, we have

$$\overset{\nabla}{\underline{\underline{C}}}_{e_i}^{-1} + \frac{1}{2\lambda}\{\underline{\underline{\hat{C}}}_{e_i}^{-1} - \underline{\underline{\hat{C}}}_{e_i}\} \times \underline{\underline{C}}_{e_i}^{-1} = \underline{\underline{0}}$$
$$\underline{\underline{\tau}}_i = G\underline{\underline{C}}_{e_i}^{-1} \quad (15)$$

$$\frac{\partial}{\partial t}\kappa_{e_i} = \dot{\varepsilon}\kappa_{e_i} - \frac{\kappa_{e_i}}{6\lambda_i}(\kappa_{e_i}^2 + \kappa_{e_i}^{-1})(1 + \kappa_{e_i}^{-1}) \quad (16)$$

The elongational viscosity is in this form:

$$\eta_e^+(\dot{\varepsilon}, t) = \sum_i \frac{\eta_i}{\dot{\varepsilon}\lambda_i}[\kappa_{e_i}^2(\dot{\varepsilon}, t) + \kappa_{e_i}^{-1}(\dot{\varepsilon}, t)] \quad (17)$$

The discrete spectrum (η_i, λ_i), characteristic of a polymer studied is determined directly by its dynamic behavior. The expressions of the dynamic moduli for Maxwell model are

$$\begin{cases} G'(\omega) = \sum_i \dfrac{\eta_i\lambda_i\omega^2}{1 + \omega^2\lambda_i^2} \\ G''(\omega) = \sum_i \dfrac{\eta_i\omega}{1 + \omega^2\lambda_i^2} \end{cases} \quad (18)$$

Thus, with dynamic measurements and the Leonov model, it is possible to calculate the rheological behavior for an extensional flow without adjustable parameters.

EXPERIMENTAL

Approach

Generally, a multifunctional coagent or monomer can be used for limiting the degradation of PP. In a preceding study we have shown, with a molecular model of PP (squalane), the efficiency of butyl acrylate monomer to limit the β-scission.[19] Moreover, in the case of trifunctional monomer such as trimethylol propane triacrylate (TMPTA), we obtained an important gel fraction ($\approx$ 70%).

First we tested the efficiency of the TMPTA with PP for limiting the degradation and to create the branched structure. The elongational measurement of polymers in this case showed a little strain hardening. Unfortunately, the chain degradation induced by the peroxide is important. Although this monomer allows us to create a grafted structure, it does not sufficiently limit the degradation of the chains. We therefore envisaged use of PP/PE blends for reduction of degradation.[20]

Blends Preparation

Blends were prepared with a Werner & Pfleiderer ZSK 30 corotating twin screw extruder with a 42 : 1 length-to-diameter ratio. For all blends, we used the same screw configuration. The total feeding rate of polymer was 5 kg/h, and the screw rotating speed 150 rpm. The temperature in the first zone was set at 160°C, and 210°C for the die. A devolatilization zone was placed prior to the pumping zone close to a die. Extrudates were cooled in water and then pelletized.

Polymers were unstabilized powder supplied by Solvay:

- PP homopolymer: PP ELTEX® HL 001 P;
- PE: PE ELTEX® A 1050 P.

The free radical initiator was 2,5-dimethyl-2,5-di(*tert*-butylperoxy)hexane (DHBP). TMPTA (Aldrich) was used as a monomer. All products were used without further purification.

The mechanical blends (M) were realized with the following values of weight fraction of PE: 10, 15, 20, and 25%. The reactive blends (R) were realized with these mechanical blends by addition of DHBP and TMPTA monomer directly in the feeding zone (Table II).

Rheological Measurements

The dynamic measurements were carried out on a Rheometrics 605 mechanical spectrometer using a parallel-plate geometry (radii of sample, 12.5 and 25 mm). The experiments were carried out in the temperature range 180–220°C, and data at different temperatures were reduced to 180°C using time–temperature superposition. The working temperature was measured, with a precision of $\pm$0.1°C, within the metallic plate in contact with the polymer melt. Depending on the temperature and frequency, the strain amplitude was taken between 2.5 and 100% to obtain a high enough value of the torque. It was always verified that the behavior of the sample was in the range of linear viscoelasticity.

The rheometer used for the elongational experiments was developed in our laboratory by R. Muller and D. Froelich.[21] The temperature was controlled with a double-walled silicon–oil bath, in which the temperature gradient was less than $\pm$0.2°C. Buoyancy prevented the sample from flowing under the effect of gravity, so that homogeneous deformation of the specimens was obtained even at very low strain rates. The specimens to be stretched in this apparatus were in a rectangular shape with typical dimensions 50 $\times$ 25 $\times$ 2.5 mm. The maximal sample deformation used was about 13. In the present study, all specimens were stretched at a temperature of 180°C and the strain rate of 0.1 s^{-1}.

Table II Formulation of PP/PE Mechanical and Reactive Blends

Ref.	PE (wt %)	Ref.	PE (wt %)	TMPTA (g/kg)	DHBP (g/kg)
M10	10	R10	10	12	0.375
M15	15	R15	15	12	0.375
M20	20	R20	20	12	0.375
M25	25	R25	25	12	0.375

Table III Molecular Weight of PP, PE, and Blends

	M_n	M_w	M_z	M_{z+1}	I_1	I_2	I_3
PP	30,000	324,000	1,320,000	3,214,000	10.8	4.1	2.4
PE	18,000	93,000	331,000	764,000	5.1	3.6	2.3
M10	29,000	250,000	809,000	1,694,000	8.6	3.2	2.1
M20	29,000	243,000	757,000	1,393,000	8.4	3.1	1.8
R10	25,000	153,000	671,000	1,713,000	6.1	4.4	2.6
R20	28,000	174,000	856,000	2,023,000	6.3	4.9	2.4

Determination by GPC at 135°C with 1,2,4 trichlorobenzene.

Thermal Analysis

The thermal behavior of the different blends was determined using a differential scanning calorimeter (Perkin–Elmer DSC4) with the following procedure: the samples (10 mg) encapsulated in aluminum pans, were heated from 50 to 200°C at 10°C/min, held 3 min at this temperature, and then cooled to 50°C at the same rate.

RESULTS AND DISCUSSION

Molecular Weight

The molecular weight distributions of polymers PP and PE and two blends (10 and 20%) were analyzed by gel permeation chromatography. 1,2,4 Trichlorobenzene, at 135°C, was used as solvent for a polymer concentration of 1 g/L. Irganox 1010, 0.5 g/L, was added to samples to prevent degradation. The molecular weight values obtained are given in Table III.

The analysis of these values shows that without stabilization, the preparation of mechanical blends gives low degradation. For $\bar{M}_w$, we found a loss of 17 and 13%, respectively, for the mechanical blends at 10 and 20% PE. For the reactive blends, we obtained a diminution of, respectively, 49 and 37% for PE contents of 10 and 20%. The molecular weight diminution is inversely proportional to the PE concentration; this confirms its stabilizing role. Moreover, we observed an increase of polydispersity $\bar{M}_z/\bar{M}_w$ and $\bar{M}_{z+1}/\bar{M}_z$ consecutive with the creation of chains of high molecular weight (Fig. 2). The peak associated with the high molecular weight represents 1.2% and 2.29% of the totality of the polymer mass for 10 and 20% PE, respectively. The gel content of all reactive blends was determined by extraction in xylene (Soxhlet) for 24 h. In all cases, the blends are gel-free. Thus the formation of the high-molecular-

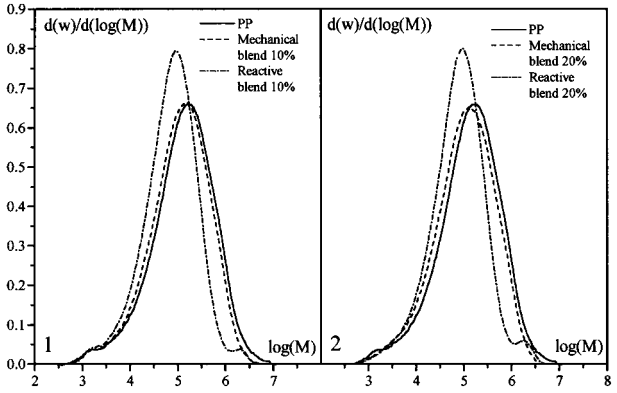

Figure 2 Molecular weight distribution: (1) PP and PP/PE blends at 10%; (2) PP and PP/PE blends at 20%.

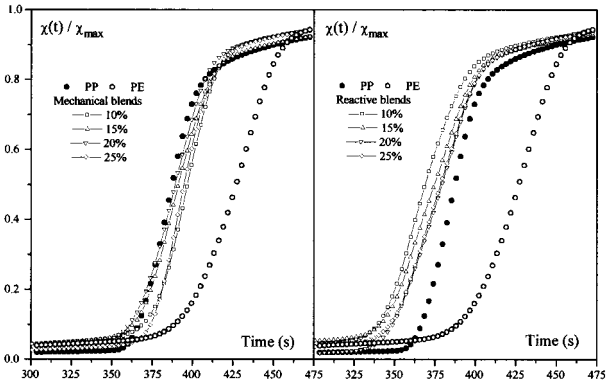

Figure 3 Crystallization: variation of degree of crystallinity versus time. Reactive and mechanical PP/PE blends.

Table IV Crystallization Rate of PP, PE, and Blends

	PP : 0.0205 s^{-1}	PE : 0.0142 s^{-1}
PE %	Mechanical (s^{-1})	Reactive (s^{-1})
10	0.0193	0.0150
15	0.0170	0.0139
20	0.0170	0.0144
25	0.0206	0.0144

weight species is not due to crosslinking of the PE phase.

The TMPTA allowed the creation of branched structure from that destroyed by β-scission. The macroradical PP is stabilized by the monomer and favors the recombination of these radicals.

Thermal Analysis

The thermograms obtained for these blends give only one exotherm peak for crystallization and two endotherm peaks for melt: one for PP phase and one for PE phase.

We represented the crystallization kinetics as a function of time for PE and PP as well as for reactive and mechanical blends (Fig. 3). The kinetics curves $\chi(t)/\chi_{max}$ show that the crystallization of mechanical blends begins before the PP,

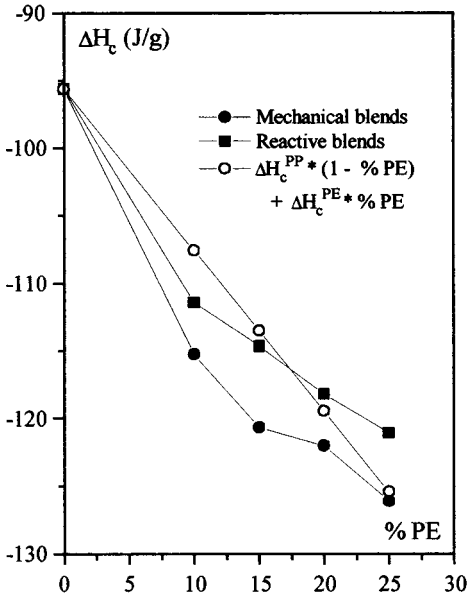

Figure 4 Crystallization enthalpy versus weight fraction in PE for reactive and mechanical PP/PE blends.

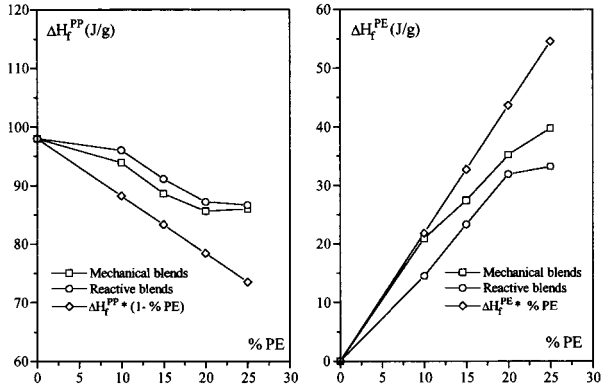

Figure 5 Melt enthalpy versus weight fraction in PE for reactive and mechanical PP/PE blends.

whereas the crystallization of reactive blends begins and is always higher than the PP. Thus we have, for the reactive blends, a nucleation phenomenon due to the presence of high-molecular-weight chains. We observed for the nonreactive blends that the maximal crystallization speed is imposed by the PP phase. For the reactive blends, this speed is imposed by the PE phase (Table IV). This phenomenon can be explained by the presence of PP–PE copolymer at the interface of PE inclusions.

This point can be confirmed by the analysis of melt and crystallization enthalpy (Figs. 4 and 5). We observe that the chemical modification induces a diminution of the crystallization enthalpy of blends.

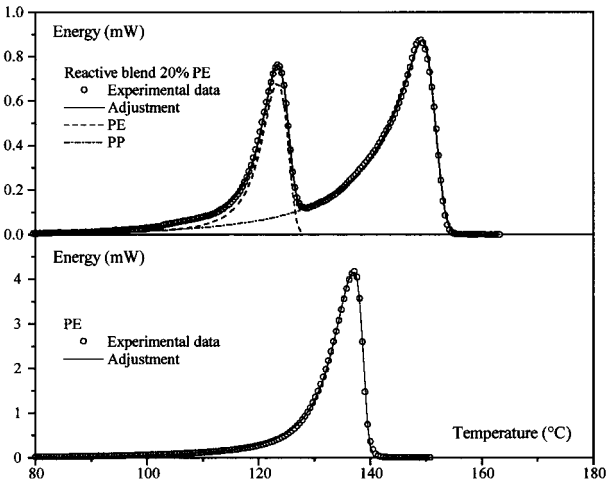

Figure 6 Melt thermograms at 10°C/min of PP/PE reactive blend (25% PE) and PE.

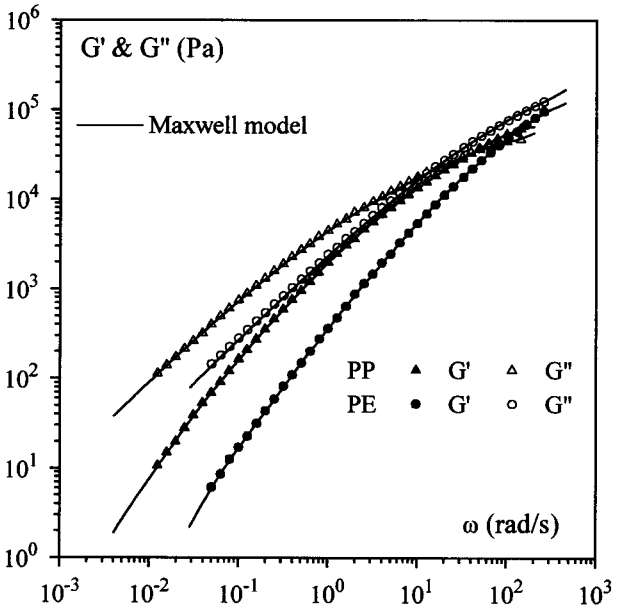

Figure 7 Dynamic moduli versus oscillation rates at 180°C for PP HL001 P and PEA1050 P.

The analysis of the melt enthalpy implies separate effects of each phase. For that, we propose the following adjustment of the thermograms:

$$Q(T) = \left[y_1 + \frac{\alpha_1 \omega_1}{\pi(\omega_1^2 + 4(T - T_{f_{PE}})^2)} \right] \times \left[1 + \text{erf}\left(\frac{T_{f_{PE}} - T}{\beta_1} \right) \right] + \left[y_2 + \frac{\alpha_2 \omega_2}{\pi(\omega_2^2 + 4(T - T_{f_{PP}})^2)} \right] \times \left[1 + \text{erf}\left(\frac{T_{f_{PP}} - T}{\beta_2} \right) \right]$$

Figure 6 shows, for PE and a reactive blend with 25% PE, that the adjustment of the thermograms is correct. The enthalpy variation of each phase versus PE fraction is given in Figure 5. We observe that chemical modification disrupts the fusion of the PE phase more than that of the PP phase.

Rheological Behavior

The viscoelastic behavior of phases is characteristic of the polymer melt near the terminal zone (Fig. 7):

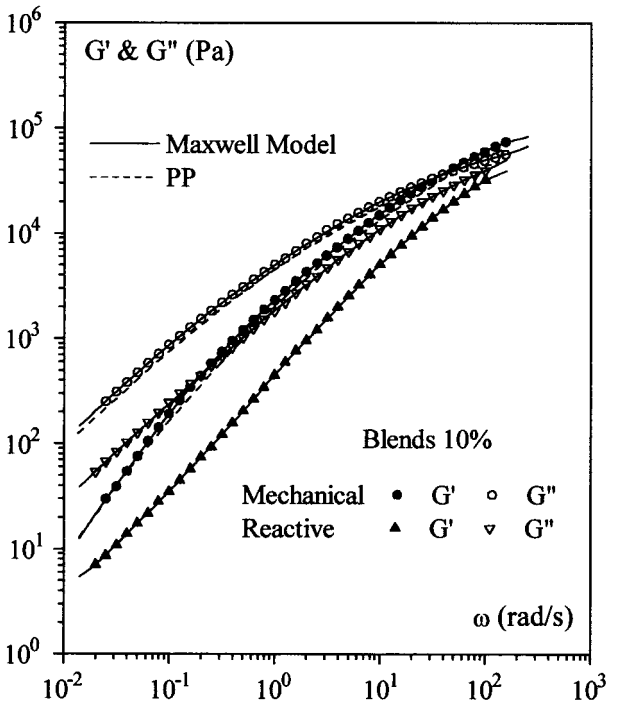

Figure 8 Dynamic moduli versus oscillation rates at 180°C for reactive and mechanical PP/PE blends (10% PE).

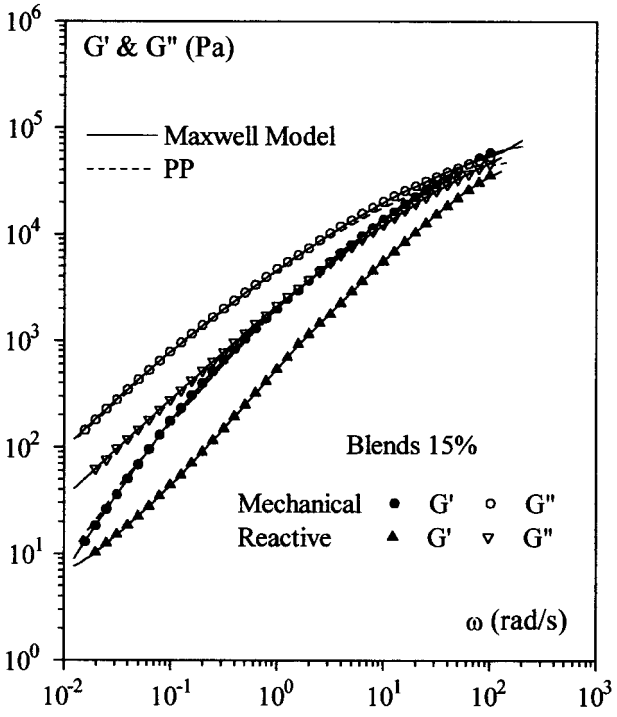

Figure 9 Dynamic moduli versus oscillation rates at 180°C for reactive and mechanical PP/PE blends (15% PE).

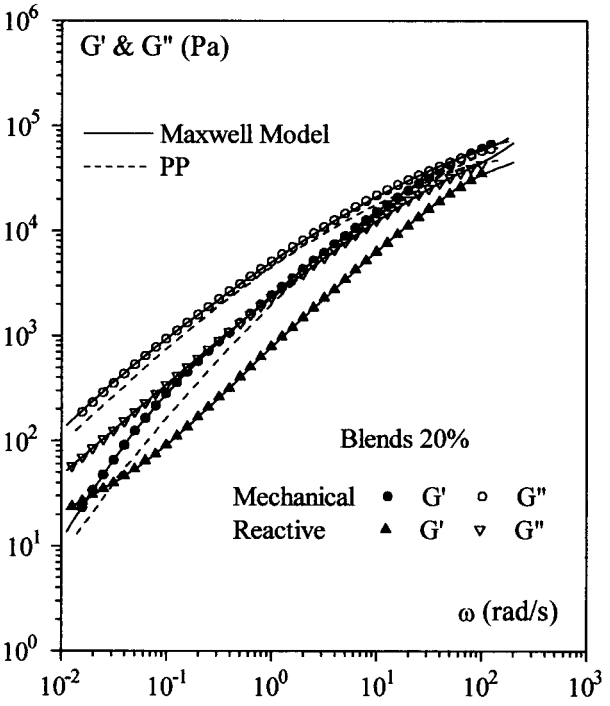

Figure 10 Dynamic moduli versus oscillation rates at 180°C for reactive and mechanical PP/PE blends (20% PE).

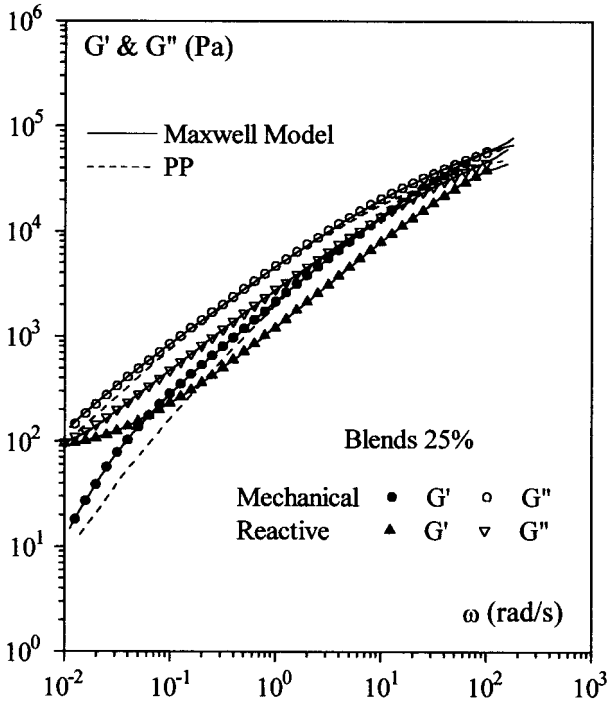

Figure 11 Dynamic moduli versus oscillation rates at 180°C for reactive and mechanical PP/PE blends (25% PE).

- PE: $G' \propto \omega^1$, $G'' \propto \omega^{1.40}$;
- PP: $G' \propto \omega^1$, $G'' \propto \omega^{1.42}$.

In the case of reactive blends, the degradation of the PP matrix induces a translation of the dynamic moduli at high oscillation rates (Figs. 8–11).

Reactive blends, compared with mechanical blends ($\tau_w \sim 5$ s), show an increase of the terminal relaxation time. At 20 and 25% of PE, we see clearly the beginning of a second elastic plateau. For a polymer melt, the relaxation time is a function of the size of the macromolecule. Thus the connected structure increases this time. We observe exactly this phenomenon with reactive blends and we assume that is due to the creation of long side chains. This point is in accordance with the gel permeation chromatography (GPC) results.

For each material, the elongational viscosity is represented by two curves: the experimental data and the results of the simulation from the dynamic moduli with Leonov model (Figs. 12–16). The discrete relaxation spectrum (η_i, λ_i) with 10 relaxation times per decade has been determined by adjusting the experimental $G'(\omega)$ and $G''(\omega)$ data (least square method) (Figs. 7–11).

For all reactive blends, we obtained strain hardening. The growth of viscosity is more important when the PE fraction is higher. In accordance with the GPC and viscoelastic results, we observe a degradation of the PP phase. In accordance with the Lodge model, the strain hardening is obtained at $\dot{\varepsilon} = 0.1\ s^{-1}$ for a polymer characterized by a terminal relaxation time $\tau_w \geq \dfrac{1}{2\dot{\varepsilon}} \rightarrow \tau_w \geq 5$ s.

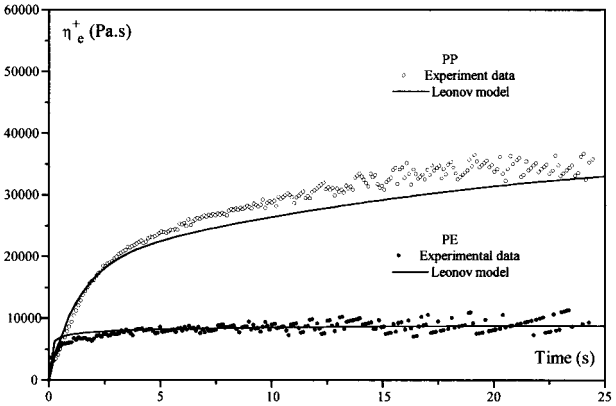

Figure 12 Elongation viscosity versus time for $\dot{\varepsilon} = 10^{-1}\ s^{-1}$ at 180°C for PP and PE.

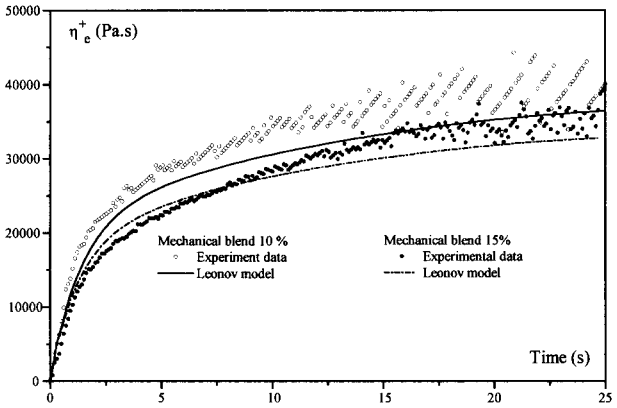

Figure 13 Elongation viscosity versus time for $\dot{\varepsilon} = 10^{-1}$ s^{-1} at 180°C for mechanical PP/PE blends (10, 15% PE). Comparison between experimental data and Leonov model.

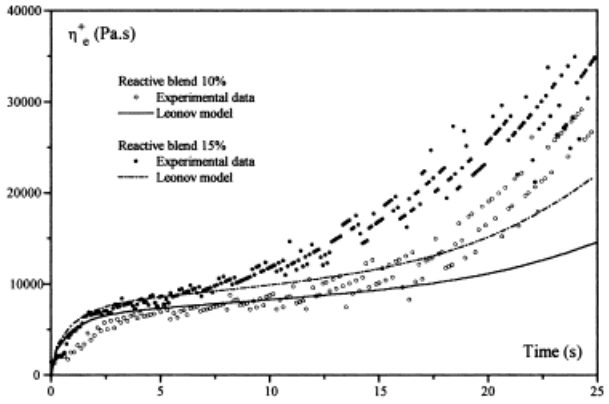

Figure 15 Elongation viscosity versus time for $\dot{\varepsilon} = 10^{-1}$ s^{-1} at 180°C for reactive PP/PE blends (10, 15% PE). Comparison between experimental data and Leonov model.

The Leonov model gives a correct description of the elongational viscosity of blends without adjusted parameters as in the Johnson and Segalman model.[22] Moreover, with this model we observed underestimation of the elongational viscosity that is due to the dynamic measurements. Thus the small range of oscillation rates accessible for these experiments did not allow us to obtain the terminal relaxation time of blends. The divergence between experimental data and model for the reactive blends with 20 and 25% PE for, respectively, times greater than 15 and 20 s can be explained by a slip of the sample in the jaws.

CONCLUSIONS

In this study we have prepared, by a reactive extrusion process, a PP characterized by strain hardening in extensional flow. This rheological behavior imposes a structural modification of the PP macromolecule: linear to long side branches.

Reactive extrusion allows one to obtain modified PP by radical chemistry, but this modification is accompanied by an important degradation of chains: β-scission. We used a polyfunctional monomer (TMPTA) associated with addition of PE to limit this degradation and build a connected structure. With GPC measurements, we confirmed the presence of high-molecular-weight species, and the thermal analysis allowed us to confirm the creation of copolymer PP/PE at the interface of the PE inclusions.

Under these conditions, all the reactive blends provide strain hardening. The elongational viscos-

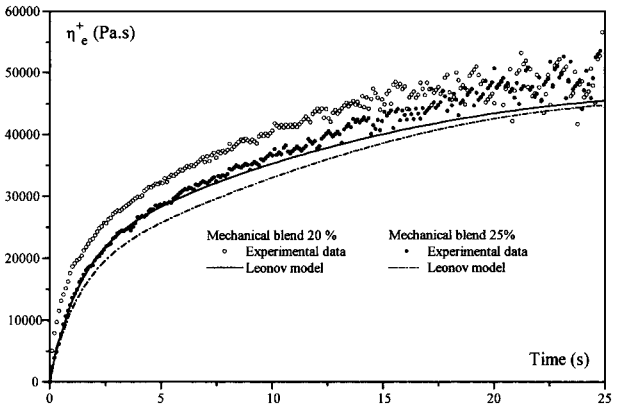

Figure 14 Elongation viscosity versus time for $\dot{\varepsilon} = 10^{-1}$ s^{-1} at 180°C for mechanical PP/PE blends (20, 25% PE). Comparison between experimental data and Leonov model.

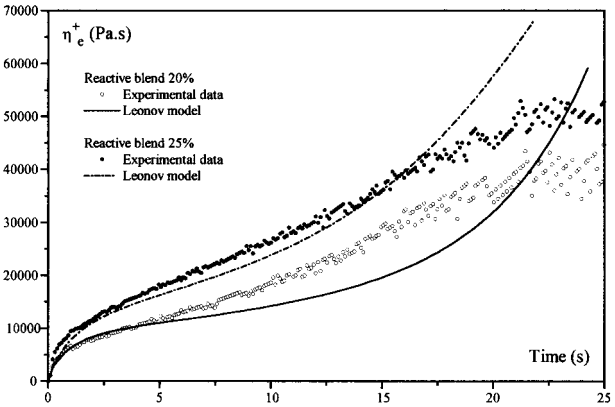

Figure 16 Elongation viscosity versus time for $\dot{\varepsilon} = 10^{-1}$ s^{-1} at 180°C for reactive PP/PE blends (20, 25% PE). Comparison between experimental data and Leonov model.

ity of all blends can be described by the Leonov model. This model gives a good description of the viscosity without adjusting parameters.

REFERENCES

1. J. J. Flat, Ph.D. Thesis, Université Louis Pasteur, Strasbourg, France, 1991.
2. G. H. Hu, J. J. Flat, and M. Lambla, *Antec '94,* 2755 (1994).
3. E. Borsig, A. Fiedlerova, and M. Lazar, *J. Macromol. Sci., Chem.,* **A16**(2), 513 (1981).
4. A. J. De Nicola, European Pat. Appl. EP-A 0 384 431 (1990) (Himont Inc.).
5. D. W. Yu, M. Xanthos, and C. G. Gogos, *Adv. Polym. Tech.,* **10**(3), 163 (1990).
6. I. Chodak, I. Janigova, and A. Romanov, *Makromol. Chem.,* **192,** 2791 (1991).
7. E. Borsig, A. Fiedlerova, L. Rychla, M. Lazar, M. Rätzsch, and G. Haudel, *J. Appl. Polym. Sci.,* **37,** 467 (1989).
8. M. J. Yoo and D. Done, *Antec '92,* 569 (1992).
9. M. R. Drickman and K. E. McHugh, *Antec '92,* 496 (1992).
10. E. M. Phillips, K. E. McHugh, K. Ogale, and M. B. Bradley, *Kunstoffe German Plastic,* **82**(8), 23 (1992).
11. R. Hingmann and B. L. Marczinke, *J. Rheol.,* **38**(3), 573 (1994).
12. N. G. Gaylord, L. Katz, and J. P. Park, Patent WO 91/13933 (1991) (to The James River Corporation).
13. A. I. Leonov, *Rheol. Acta,* **15,** 85 (1976).
14. A. I. Leonov, E. H. Lipkina, E. D. Paskhin, and A. N. Prokunin, *Rheol. Acta,* **15,** 411 (1976).
15. A. I. Leonov and A. N. Prokunin, *Rheol. Acta,* **19,** 393 (1980).
16. A. I. Leonov, *Rheol. Acta,* **21,** 683 (1982).
17. A. I. Leonov and A. N. Prokunin, *Rheol. Acta,* **22,** 137 (1983).
18. A. I. Leonov, *J. Non-Newtonian Fluid Mech.,* **25,** 1 (1987).
19. S. Drillières, D. Graebling, and R. Mestanza, *Polymer Processing Society European Meeting,* Strasbourg, France (1994).
20. M. Lambla and D. Graebling, European Patent EP 0 686 664 (1995) (to Solvay S. A.).
21. R. Muller and D. Froelich, *Polymer,* **26,** 1477 (1984).
22. M. W. Johnson and D. Segalman, *J. Non-Newtonian Fluid Mech.,* **2,** 255 (1977).